IEEE Access
Multidisciplinary : Rapid Review : Open Access Journal

Received February 21, 2020, accepted April 6, 2020, date of publication April 10, 2020, date of current version April 29, 2020.

Digital Object Identifier 10.1109/ACCESS.2020.2987068

Multiuser Space–Time Line Code With Transmit Antenna Selection

JINGON JOUNG[1], (Senior Member, IEEE), AND JIHOON CHOI[2], (Senior Member, IEEE)
[1]School of Electrical and Electronics Engineering, Chung-Ang University, Seoul 06974, South Korea
[2]School of Electronics and Information Engineering, Korea Aerospace University, Goyang 10540, South Korea

Corresponding author: Jihoon Choi (jihoon@kau.ac.kr)

This work was supported by the National Research Foundation of Korea (NRF) Grant funded by the Korean Government (MSIT) under Grant 2018R1A4A1023826 and Grant NRF-2019R1A2C1084168.

ABSTRACT In this paper, a multiuser space-time line code (MU-STLC) scheme is newly designed that concurrently delivers multiple STLC signals to multiple users, and a preprocessing matrix for the MU-STLC is derived based on the minimum mean square error criterion. The novel MU-STLC method retains the conventional STLC receiver structure so that each user linearly combines the received signals without using the full channel state information to decode the STLC signals. With more transmit antennas than the number of users having two receive antennas, a transmit antenna selection (TAS) scheme is investigated in combination with the proposed MU-STLC method, and the detection signal-to-interference-plus-noise ratio (SINR) is derived depending on a specific TAS pattern. The performance improvement obtained from the TAS is significant, yet finding the optimal TAS pattern is a combinatorial problem that requires prohibitively high computational complexity. To resolve this issue, a greedy TAS algorithm is also proposed that iteratively selects the transmit antenna maximizing the detection SINR in each greedy step. The numerical results verify the efficacy of the proposed MU-STLC system with the SINR-based greedy TAS algorithm in terms of the bit error rate performance and computational complexity. For example, comparing with a scheme that selects four antennas from eight antennas randomly to support four users, the proposed TAS scheme can reduce the required signal-to-noise ratio for achieving 10^{-3} bit-error-rate by approximately 6 *dB* when quadrature phase-shift keying is employed. Furthermore, the proposed method can achieve comparable performance to the optimal antenna selection scheme with the reduced computational complexity by $\mathcal{O}(M^5)$ from $\mathcal{O}(M^{U+3})$, where M and U are the numbers of transmit antennas and selected antennas (or users), respectively.

INDEX TERMS Space-time line code, multiuser, transmit antenna selection, greedy algorithm.

I. INTRODUCTION

Recently, a new full-rate full-spatial diversity achieving scheme, called space–time line code (STLC), was proposed in [1], [2]. The STLC scheme is fully symmetric with the space–time block code (STBC) [3]–[5], also known as Alamouti code [6], based on the reciprocity between a transmitter and a receiver. Precisely, an $M \times N$ STLC system with M-transmit and N-receive antennas is symmetric with an $N \times M$ STBC system that has N-transmit and M-receive antennas, where $M \geq 1$ and $N \in \{2, 3, 4\}$. Under the symmetric channel state information (CSI) conditions, i.e., full CSI is required at a transmitter for STLC whereas, at a receiver for STBC, the full spatial-diversity gain is achieved at both systems. The STLC can be interpreted as a precoded STBC using CSI at the transmitter (i.e., CSIT) so that CSI is not necessarily required at the STLC receiver (see Section II). Contrary to the STBC, the STLC can be readily scaled up to an arbitrarily large number of transmit antennas. Moreover, whereas an optimal beamforming scheme with CSIT requires a complexity order of $\mathcal{O}(M^3)$ for finding the dominant singular vector, the complexity of the STLC linearly increases with the number of transmit antennas, $\mathcal{O}(\mathcal{M})$, and the STLC scheme is more robust against the CSI uncertainty [2]. By the *low-complexity* linear processing for STLC encoding and decoding, *scalability* of the number of transmit antennas, and *robustness* against the CSI uncertainty, the STLC scheme has been applied to various communication systems requiring CSIT, such as multiuser systems [2], [7], two-way relay systems [8], [9], antenna shuffling systems [10], and machine learning-based blind decoding systems [11]. The spatial-domain coding in STLC was applied to a frequency

The associate editor coordinating the review of this manuscript and approving it for publication was Luyu Zhao.

domain in an orthogonal-frequency division multiplexing system, and the efficacy of STLC was investigated [12]. Since the STLC allows a semi-blind detection at the receiver without full CSI, the STLC transmitter does not need to broadcast a long training or pilot sequence for channel estimation at the receiver, which prevents an unauthorized intruder, i.e., an eavesdropper, from estimating the channels, resulting in an improvement of the physical-layer security [13].

The conventional single-stream STLC was extended to a double STLC that could transmit two STLC streams for point-to-point communications in [14]. The two STLC streams can be separately transferred to two users, i.e., it works as a two-user STLC system. The double STLC scheme minimizes the inter-stream interference based on the minimum mean square error (MMSE) criterion; however, its design is not scalable to multiple users more than two. On the other hand, a multiuser-STLC scheme in [2] and [7] can support an arbitrary number of users. However, these schemes simultaneously transmit multiple data streams without considering multiuser (inter-stream) interferences, thus a large number of transmit antennas are required to suppress the multiuser interferences for reliable communications.

In this study, we derive a multiuser-STLC (MU-STLC) scheme, which can deliver *multiple* STLC streams to *multiple* users. Owing to the STLC schemes can provide energy efficiency improvement at the receiver [8], the proposed multiuser-STLC (MU-STLC) scheme can be applicable to a system supporting multiple power/energy-limited devices, simultaneously. For the proposed MU-STLC transmission, the transmitter uses a preprocessing matrix designed in the minimum mean square error (MMSE) sense based on the CSI, and each user having two receive antennas decodes its STLC signal, utilizing the low-complexity STLC combining structure. The existing STLC and double STLC schemes can transfer one and two data streams, respectively. In contrast, the proposed MU-STLC method can increase the number of concurrently transmitted data streams up to the number of users U reducing the inter-stream interferences in the MMSE sense, when $M \geq U$. The proposed MU-STLC can support multi-stream transmission for multiple users through preprocessing at the transmitter without changing the receivers, i.e. the conventional low-complexity STLC decoder is used for user receivers.

Furthermore, a transmit antenna selection (TAS) scheme is proposed to improve the signal-to-interference-plus-noise ratio (SINR) at each user. A TAS scheme alleviates the implementation cost of RF chains for multiple-input multiple-output (MIMO) systems retaining the spatial multiplexing and diversity gain. For example, a multimode TAS method allows any number of data streams to be dynamically selected providing array gain [15], and the feedback rate can be reduced for TAS with Alamouti coding [16]. Also, TAS methods can be combined with a wire-tap channel without CSIT, a massive MIMO channel, and a non-orthogonal multiple access system for secure communications [17]–[19], and the use of TAS has been investigated

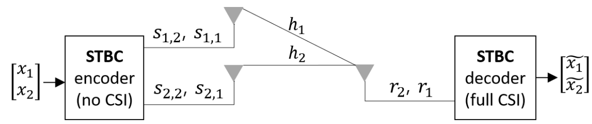

FIGURE 1. 2×1 system with space–time block code (STBC) in [6].

in spatial modulation and millimeter wave MIMO systems for performance enhancement [20], [21]. In an MU-STLC system, TAS is performed by finding the antenna subset minimizing the mean square error (MSE) (or equivalently maximizing the detection SINR), and the optimal TAS design requires $\mathcal{O}(M^{U+3})$ computational complexity which is prohibitively large especially when M and/or U is large. In an attempt to reduce the complexity, an SINR-based greedy TAS algorithm is proposed. Through complexity analysis, it is shown that the complexity order of the proposed TAS method is $O(M^5)$. Through numerical simulations, the complexity analysis is confirmed, and it is verified that the proposed MU-STLC with SINR-based greedy TAS can achieve near-optimal bit-error-rate (BER) performance with a noticeably reduced computational load. For example, comparing with a scheme that selects four antennas from eight antennas randomly to support four users, namely, $M = 8$ and $U = 4$, the proposed TAS scheme can reduce the required signal-to-noise ratio (SNR) for achieving 10^{-3} BER by approximately 6 *dB* when quadrature phase-shift keying (QPSK) is employed.

Notations: Superscripts T, H, $*$, and -1 denote transposition, Hermitian transposition, complex conjugate, and inversion, respectively, for any scalar, vector, or matrix. The notations $|x|$ and $\|\boldsymbol{X}\|_F$ denote the absolute value of x and the Frobenius-norm of matrix $\boldsymbol{X}$, respectively; $\boldsymbol{I}_m$ and $\boldsymbol{0}_m$ represent an m-by-m identity matrix and a zero matrix, respectively; $\mathrm{tr}(\boldsymbol{A})$ is the trace operation of matrix $\boldsymbol{A}$; $\mathrm{blkdiag}(\boldsymbol{X}_1 \cdots \boldsymbol{X}_a)$ returns a block diagonal matrix whose main diagonal matrices are $\boldsymbol{X}_1 \cdots \boldsymbol{X}_a$; and $x \sim \mathcal{CN}(0, \sigma^2)$ means that a complex random variable x conforms to a complex normal distribution with a zero mean and variance σ^2. $\mathrm{E}[x]$ stands for the expectation of random variable x.

II. REVIEW AND COMPARISON OF SINGLE-USER STBC AND STLC SYSTEMS

We briefly introduce a 2×1 STBC system in [6] and a 1×2 STLC system in [1] to clarify the difference between them and to describe the encoding and decoding procedure of a 1×2 STLC method which is extended to the new $M \times 2U$ MU-STLC system.

A. 2×1 STBC SYSTEM

As shown in Fig. 1, two information symbols x_1 and x_2 with $\mathrm{E}[|x|^2] = 1$ are encoded as [6]

$$\begin{bmatrix} s_{1,1} & s_{1,2} \\ s_{2,1} & s_{2,2} \end{bmatrix} = \frac{1}{\sqrt{2}} \begin{bmatrix} x_1 & -x_2^* \\ x_2 & x_1^* \end{bmatrix}, \tag{1}$$

where $s_{m,t}$ is the STBC symbols transmitted at the mth antenna and time t. The receiver rearranges the received

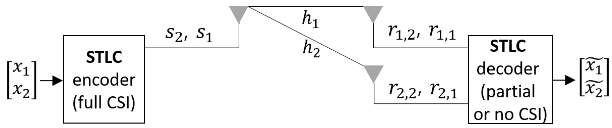

FIGURE 2. 1 × 2 system with space–time line code (STLC) in [1].

signals r_1 and r_2 and then decodes the transmit symbols x_1 and x_2 using the orthogonality of the STBC encoded symbols in (1). The decoding SNR of STBC is given by

$$\rho_{STBC} = \frac{\gamma}{2\sigma_z^2}, \tag{2}$$

where $\gamma = |h_1|^2 + |h_2|^2$ is the effective channel gain and σ_z^2 is the per-antenna noise variance. Here, note that full diversity gain is achieved by using full CSI at the STBC receiver.

B. ALTERNATIVE FORM OF 1×2 STLC SYSTEM

When we use a type-five STLC structure in [1, Table 4], the alternative model of 1×2 STLC shown in Fig. 2 is given by [14]

$$\begin{bmatrix} s_1 & s_2 \end{bmatrix} = \frac{1}{\sqrt{\gamma}} \boldsymbol{h}^H \begin{bmatrix} x_1 & -x_2^* \\ x_2 & x_1^* \end{bmatrix}, \tag{3}$$

where s_t is the STLC symbol transmitted at time t and $\boldsymbol{h} = \begin{bmatrix} h_1 \ h_2 \end{bmatrix}^T \in \mathbb{C}^{2\times 1}$ is the channel vector. Denoting $r_{n,t}$ is the received signal at antenna n at time t, the four received signals are then written in a matrix form as follows:

$$\begin{aligned} \begin{bmatrix} r_{1,1} & r_{1,2} \\ r_{2,1} & r_{2,2} \end{bmatrix} &= \begin{bmatrix} \boldsymbol{r}_1 & \boldsymbol{r}_2 \end{bmatrix} \\ &= \boldsymbol{h} \begin{bmatrix} s_1 & s_2 \end{bmatrix} + \boldsymbol{Z} \in \mathbb{C}^{2\times 2}, \end{aligned} \tag{4}$$

where $\boldsymbol{r}_t \in \mathbb{C}^{2\times 1}$ is the received signal vector at time t; $\boldsymbol{Z} = \begin{bmatrix} \boldsymbol{z}_1 \ \boldsymbol{z}_2 \end{bmatrix} \in \mathbb{C}^{2\times 2}$ is a noise matrix whose (n, t)th element $z_{n,t}$ is the AWGN at $r_{n,t}$ distributed with $\mathcal{CN}(0, \sigma_z^2)$.

By stacking $\boldsymbol{r}_1 = \begin{bmatrix} r_{1,1} \ r_{2,1} \end{bmatrix}^T$ on the conjugate of $\boldsymbol{r}_2 = \begin{bmatrix} r_{1,2} \ r_{2,2} \end{bmatrix}^T$, we construct the alternative form of the received signal vector as follows:

$$\begin{aligned} \begin{bmatrix} \boldsymbol{r}_1 \\ \boldsymbol{r}_2^* \end{bmatrix} &= \begin{bmatrix} r_{1,1} \\ r_{2,1} \\ r_{1,2}^* \\ r_{2,2}^* \end{bmatrix} = \frac{1}{\sqrt{\gamma}} \begin{bmatrix} h_1 \ h_1^* & h_1 h_2^* \\ h_2 \ h_1^* & h_2 \ h_2^* \\ (h_1 h_2^*)^* & -(h_1 \ h_1^*)^* \\ (h_2 h_2^*)^* & -(h_2 h_1^*)^* \end{bmatrix} \begin{bmatrix} x_1 \\ x_2 \end{bmatrix} + \begin{bmatrix} z_1 \\ z_2^* \end{bmatrix} \\ &= \frac{1}{\sqrt{\gamma}} \begin{bmatrix} \boldsymbol{h}\boldsymbol{h}^H \\ (\boldsymbol{h}\boldsymbol{h}^H)^* \boldsymbol{Q}_2 \end{bmatrix} \boldsymbol{x} + \boldsymbol{z} \in \mathbb{C}^{4\times 1}, \end{aligned} \tag{5}$$

where $\boldsymbol{Q}_2 = \left[\begin{smallmatrix} 0 & -1 \\ 1 & 0 \end{smallmatrix}\right]$, $\boldsymbol{x} = \left[\begin{smallmatrix} x_1 \\ x_2 \end{smallmatrix}\right]$, and $\boldsymbol{z} = \left[\begin{smallmatrix} z_1 \\ z_2^* \end{smallmatrix}\right]$. Using (5), the STLC combining procedure can be represented as below [14]:

$$\begin{aligned} \begin{bmatrix} \boldsymbol{I}_2 & \boldsymbol{Q}_2^T \end{bmatrix} \begin{bmatrix} \boldsymbol{r}_1 \\ \boldsymbol{r}_2^* \end{bmatrix} &= \boldsymbol{r}_1 + \boldsymbol{Q}_2^T \boldsymbol{r}_2^* \\ &= \frac{1}{\sqrt{\gamma}} \left(\boldsymbol{h}\boldsymbol{h}^H + \boldsymbol{Q}_2^T (\boldsymbol{h}\boldsymbol{h}^H)^* \boldsymbol{Q}_2 \right) \boldsymbol{x} + \boldsymbol{z}' \\ &= \sqrt{\gamma}\boldsymbol{x} + \boldsymbol{z}' \in \mathbb{C}^{2\times 1}, \end{aligned} \tag{6}$$

where $\boldsymbol{z}' = \boldsymbol{z}_1 + \boldsymbol{Q}_2^T \boldsymbol{z}_2^*$ and $\mathrm{E}[\boldsymbol{z}'(\boldsymbol{z}')^H] = 2\sigma_z^2 \boldsymbol{I}_2$.

The resulting decoding SNR after the STLC combining is readily derived from (6) as

$$\rho_{STLC} = \frac{\gamma}{2\sigma_z^2}, \tag{7}$$

which is identical to the decoding SNR of STBC in (2). From (7), it is verified that 1×2 STLC achieves the same performance as 2×1 STBC in terms of the diversity gain and array gain. Note that only partial CSI γ is required at the STLC receiver. We extend the alternative model of 1×2 STLC to the proposed MU-STLC supporting multiple users in the next section.

III. PROPOSED MU-STLC SYSTEM

We consider an M-by-$2U$ MU-STLC system, in which a transmitter with M-transmit antennas support U users having two receive antennas for STLC as shown in Fig. 3. Here, we assume that the transmitter has a sufficient number of antennas as $M \geq U$. Let $x_{u,t}$ be the tth modulated information symbol that is transmitted to user $u \in \mathcal{U} = \{1, 2, \ldots, U\}$, with $\mathrm{E}[|x_{u,t}|^2] = \sigma_x^2$. Then, the proposed MU-STLC signals are defined as

$$\boldsymbol{S} = \begin{bmatrix} s_{1,1} & s_{1,2} \\ \vdots & \vdots \\ s_{U,1} & s_{U,2} \end{bmatrix} = \boldsymbol{V}\boldsymbol{X} \in \mathbb{C}^{U\times 2}, \tag{8}$$

where $\boldsymbol{X} = \begin{bmatrix} \boldsymbol{X}_1 \cdots \boldsymbol{X}_u \cdots \boldsymbol{X}_U \end{bmatrix}^T \in \mathcal{C}^{2U\times 2}$ and

$$\boldsymbol{X}_u = \begin{bmatrix} x_{u,1} & x_{u,2} \\ -x_{u,2}^* & x_{u,1}^* \end{bmatrix} \in \mathbb{C}^{2\times 2}. \tag{9}$$

Here, $\boldsymbol{V} \in \mathbb{C}^{U\times 2U}$ is the MU-STLC preprocessing matrix, such that $\|\boldsymbol{V}\|_F^2 = 1$. Herein, our objective is to design an optimal preprocessing matrix, $\boldsymbol{V}$, to support multiple STLC users, who independently perform a single-user STLC decoding process in (6) to decode their information signals.[1]

The receive signals with TAS are then modeled as

$$\begin{bmatrix} \boldsymbol{r}_{1,1} & \boldsymbol{r}_{1,2} \\ \vdots & \vdots \\ \boldsymbol{r}_{U,1} & \boldsymbol{r}_{U,2} \end{bmatrix} = \boldsymbol{H}\boldsymbol{P}\boldsymbol{S} + \boldsymbol{Z} \in \mathbb{C}^{2U\times 2}, \tag{10}$$

where $\boldsymbol{r}_{u,t} \in \mathbb{C}^{2\times 1}$ is the received signal vector, whose nth element $r_{u,n,t}$ is the received signal at the nth receive antenna of user u at time t; $\boldsymbol{H} = [\boldsymbol{h}_1 \cdots \boldsymbol{h}_m \cdots \boldsymbol{h}_M]$ and $\boldsymbol{h}_m \in \mathbb{C}^{2U\times 1}$ is a channel vector between the mth transmit antenna and users, which is static for $t = 1$ and 2 and $\mathrm{E}[\boldsymbol{h}_m\boldsymbol{h}_m^H] = \boldsymbol{I}_M$; $\boldsymbol{P} = \begin{bmatrix} \boldsymbol{p}_1 \cdots \boldsymbol{p}_U \end{bmatrix}$ and $\boldsymbol{p}_k$ is an M-by-1 antenna selection vector for the kth STLC symbols, namely $s_{k,1}$ and $s_{k,2}$, whose ith element $p_{k,i} = 1$ if the ith transmit antenna is selected, and $p_{k,i} = 0$ otherwise; and $\boldsymbol{Z} \in \mathbb{C}^{2U\times 2}$ is a noise matrix whose elements are independent and identically distributed (i.i.d.) complex Gaussian random variables with zero mean

[1]Note that the STLC preprocessing matrix $\boldsymbol{V}$ in (8) enables the user to decode the STLC signals through the simple linear combining without full CSI, and the STBC structure in (9) will provide the full spatial diversity gain of the STLC users and symmetric properties to the STLC.

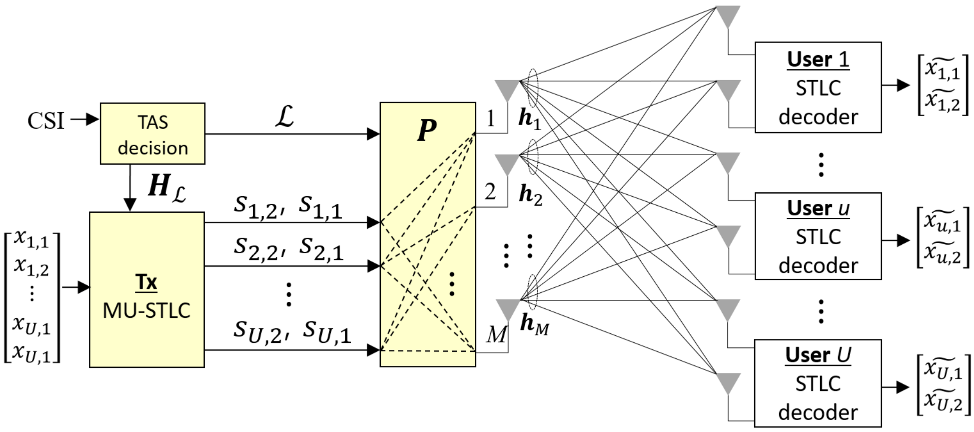

FIGURE 3. The proposed $M \times 2U$ multiuser-STLC (MU-STLC) system with a transmit antenna selection (TAS) scheme.

and variance σ_z^2. Here, $\sum_k p_{k,i} = 1, \forall i$ for the orthogonal antenna selection. If the kth antenna is selected, $\sum_i p_{k,i} = 1$, and otherwise, $\sum_i p_{k,i} = 0$.

Let $\mathcal{L} = \{i_1, \ldots, i_u, \ldots, i_U\}$ be the set of the selected antenna indices, where $i_u \in \{1, \ldots, M\}$ is the antenna index selected for user u, and $i_u \neq i_{u'}$ when $u \neq u' \in \mathcal{U}$. Then the received signals in (10) can be rewritten as

$$\boldsymbol{HPS} + \boldsymbol{Z} \triangleq \boldsymbol{H}_{\mathcal{L}}\boldsymbol{VX} + \boldsymbol{Z} \in \mathbb{C}^{2U\times 2}, \tag{11}$$

where $\boldsymbol{H}_{\mathcal{L}}$ is the selected channel matrix, which is given as

$$\boldsymbol{H}_{\mathcal{L}} = \begin{bmatrix}\boldsymbol{h}_{i_1} & \cdots & \boldsymbol{h}_{i_u} & \cdots & \boldsymbol{h}_{i_U}\end{bmatrix} \in \mathcal{C}^{2U\times U}. \tag{12}$$

For the MU-STLC decoding, (11) is alternatively reconstructed in a linear form as

$$\begin{aligned}\boldsymbol{r} &\triangleq \begin{bmatrix}\boldsymbol{r}_{1,1}^T & \cdots & \boldsymbol{r}_{U,1}^T & \boldsymbol{r}_{1,2}^H & \cdots & \boldsymbol{r}_{U,2}^H\end{bmatrix}^T \\ &= \begin{bmatrix}\boldsymbol{H}_{\mathcal{L}}\boldsymbol{V} \\ (\boldsymbol{H}_{\mathcal{L}}\boldsymbol{V})^*\boldsymbol{Q}_{2U}\end{bmatrix}\boldsymbol{x} + \boldsymbol{z} \in \mathbb{C}^{4U\times 1},\end{aligned} \tag{13}$$

where

$$\boldsymbol{x} = [x_{1,1}\ x_{1,2} \ldots x_{u,1}\ x_{u,2} \ldots x_{U,1}\ x_{U,2}]^T; \tag{14a}$$

$$\boldsymbol{Q}_{2U} = \mathrm{blkdiag}\left(\boldsymbol{Q}_2, \cdots, \boldsymbol{Q}_2\right) \in \mathcal{R}^{2U\times 2U}; \tag{14b}$$

$$\boldsymbol{Q}_2 = \begin{bmatrix}0 & -1 \\ 1 & 0\end{bmatrix}; \tag{14c}$$

and $\boldsymbol{z} \in \mathbb{C}^{4U\times 1}$ is the corresponding AWGN vector with $\mathrm{E}[\boldsymbol{z}\boldsymbol{z}^H] = \sigma_z^2\boldsymbol{I}_{4U}$.

User u performs STLC combining in (6) as $\boldsymbol{r}_{u,1} + \boldsymbol{Q}_2^T\boldsymbol{r}_{u,2}^*$; therefore, the multiuser combined-STLC received signals are represented as follows:

$$\begin{aligned}\boldsymbol{y} &= \begin{bmatrix}\boldsymbol{I}_{2U} & \boldsymbol{Q}_{2U}^T\end{bmatrix}\boldsymbol{r} \\ &= \begin{bmatrix}\boldsymbol{I}_{2U} & \boldsymbol{Q}_{2U}^T\end{bmatrix}\begin{bmatrix}\boldsymbol{H}_{\mathcal{L}}\boldsymbol{V} \\ (\boldsymbol{H}_{\mathcal{L}}\boldsymbol{V})^*\boldsymbol{Q}_{2U}\end{bmatrix}\boldsymbol{x} + \begin{bmatrix}\boldsymbol{I}_{2U} & \boldsymbol{Q}_{2U}^T\end{bmatrix}\boldsymbol{z} \\ &= \left(\boldsymbol{H}_{\mathcal{L}}\boldsymbol{V} + \boldsymbol{Q}_{2U}^T(\boldsymbol{H}_{\mathcal{L}}\boldsymbol{V})^*\boldsymbol{Q}_{2U}\right)\boldsymbol{x} + \boldsymbol{z}' \\ &= \begin{bmatrix}\boldsymbol{H}_{\mathcal{L}} & \boldsymbol{Q}_{2U}^T\boldsymbol{H}_{\mathcal{L}}^*\end{bmatrix}\begin{bmatrix}\boldsymbol{V} \\ \boldsymbol{V}^*\boldsymbol{Q}_{2U}\end{bmatrix}\boldsymbol{x} + \boldsymbol{z}' \\ &\triangleq \boldsymbol{H}_t\boldsymbol{V}_t\boldsymbol{x} + \boldsymbol{z}',\end{aligned} \tag{15}$$

where

$$\boldsymbol{H}_t \triangleq \begin{bmatrix}\boldsymbol{H}_{\mathcal{L}} & \boldsymbol{Q}_{2U}^T\boldsymbol{H}_{\mathcal{L}}^*\end{bmatrix} \in \mathbb{C}^{2U\times 2U} \tag{16a}$$

$$\boldsymbol{V}_t \triangleq \begin{bmatrix}\boldsymbol{V}^T & \boldsymbol{Q}_{2U}^T\boldsymbol{V}^H\end{bmatrix}^T \in \mathbb{C}^{2U\times 2U}, \tag{16b}$$

and the combined AWGN vector $\boldsymbol{z}' \in \mathbb{C}^{2U\times 1}$ conforms to the distribution $\mathcal{CN}(\boldsymbol{0}_{2U}, 2\sigma_z^2\boldsymbol{I}_{2U})$.

The error vector after the detection of $\boldsymbol{x}$ from (15) is then defined as

$$\begin{aligned}\boldsymbol{e} &= c\boldsymbol{y} - \boldsymbol{x} \\ &= (c\boldsymbol{H}_t\boldsymbol{V}_t - \boldsymbol{I}_{2U})\boldsymbol{x} + c\boldsymbol{z}',\end{aligned} \tag{17}$$

where $1/c$ is the real-value effective channel gain from STLC. Let us define $\boldsymbol{W}_t$ as

$$\begin{aligned}\boldsymbol{W}_t &\triangleq c\boldsymbol{V}_t \\ &= c\begin{bmatrix}\boldsymbol{V} \\ \boldsymbol{V}^*\boldsymbol{Q}_{2U}\end{bmatrix}.\end{aligned} \tag{18}$$

From the definition in (18), we can derive that

$$c = \frac{\|\boldsymbol{W}_t\|_F}{\|\boldsymbol{V}_t\|_F} = \frac{\|\boldsymbol{W}_t\|_F}{\sqrt{2}\|\boldsymbol{V}\|_F} = \frac{\|\boldsymbol{W}_t\|_F}{\sqrt{2}}, \tag{19}$$

and rewrite the error vector in (17) as

$$\boldsymbol{e} = (\boldsymbol{H}_t\boldsymbol{W}_t - \boldsymbol{I}_{2U})\boldsymbol{x} + \frac{1}{\sqrt{2}}\|\boldsymbol{W}_t\|_F\boldsymbol{z}'. \tag{20}$$

The MSE, $J(\boldsymbol{W}_t)$, is then derived as (21) at the bottom of the next page. The optimal $\boldsymbol{W}_t$ that minimizes MSE can be obtained by solving the first-order optimality condition, i.e.,

$$\begin{aligned}\frac{\partial J(\boldsymbol{W}_t)}{\partial \boldsymbol{W}_t^*} &= \sigma_x^2\boldsymbol{H}_t^H(\boldsymbol{H}_t\boldsymbol{W}_t - \boldsymbol{I}_{2U}) + 2U\sigma_z^2\boldsymbol{W}_t \\ &= \boldsymbol{0}_{2U}.\end{aligned} \tag{22}$$

From (22), the optimal $\boldsymbol{W}_t$ is obtained as follows:

$$\begin{aligned}\boldsymbol{W}_{t,o} &= \boldsymbol{H}_t^H\left(\boldsymbol{H}_t\boldsymbol{H}_t^H + \frac{2U\sigma_z^2}{\sigma_x^2}\boldsymbol{I}_{2U}\right)^{-1} \\ &= \begin{bmatrix}\boldsymbol{H}_{\mathcal{L}}^H \\ \boldsymbol{H}_{\mathcal{L}}^T\boldsymbol{Q}_{2U}\end{bmatrix}\boldsymbol{\Delta}_{\mathcal{L}},\end{aligned} \tag{23}$$

where

$$\begin{aligned}\boldsymbol{\Delta}_{\mathcal{L}} &\triangleq \left(\boldsymbol{H}_t\boldsymbol{H}_t^H + \frac{2U\sigma_z^2}{\sigma_x^2}\boldsymbol{I}_{2U}\right)^{-1}\\ &= \left(\left[\boldsymbol{H}_{\mathcal{L}}\ \boldsymbol{Q}_{2U}^T\boldsymbol{H}_{\mathcal{L}}^*\right]\begin{bmatrix}\boldsymbol{H}_{\mathcal{L}}^H\\ \boldsymbol{H}_{\mathcal{L}}^T\boldsymbol{Q}_{2U}\end{bmatrix} + \frac{2U\sigma_z^2}{\sigma_x^2}\boldsymbol{I}_{2U}\right)^{-1}\\ &= \left(\boldsymbol{H}_{\mathcal{L}}\boldsymbol{H}_{\mathcal{L}}^H + \boldsymbol{Q}_{2U}^T\boldsymbol{H}_{\mathcal{L}}^*\boldsymbol{H}_{\mathcal{L}}^T\boldsymbol{Q}_{2U} + \frac{2U\sigma_z^2}{\sigma_x^2}\boldsymbol{I}_{2U}\right)^{-1}. \quad (24)\end{aligned}$$

From (18) and (23), we obtain the following equality

$$\begin{aligned}\boldsymbol{W}_{t,o} &= \begin{bmatrix}\boldsymbol{H}_{\mathcal{L}}^H\boldsymbol{\Delta}_{\mathcal{L}}\\ \boldsymbol{H}_{\mathcal{L}}^T\boldsymbol{Q}_{2U}\boldsymbol{\Delta}_{\mathcal{L}}\end{bmatrix}\\ &= c\begin{bmatrix}\boldsymbol{V}\\ \boldsymbol{V}^*\boldsymbol{Q}_{2U}\end{bmatrix}, \quad (25)\end{aligned}$$

which shows the optimal $\boldsymbol{V}_o$, i.e., $\boldsymbol{V}_o = \frac{1}{c}\boldsymbol{H}_{\mathcal{L}}^H\boldsymbol{\Delta}_{\mathcal{L}}$. Considering the definition that $\|\boldsymbol{V}\|_F^2 = 1$, $c = \|\boldsymbol{H}_{\mathcal{L}}^H\boldsymbol{\Delta}_{\mathcal{L}}\|_F$ and the MMSE-based optimal MU-STLC preprocessing matrix $\boldsymbol{V}_o$ is obtained from (25) as

$$\boldsymbol{V}_o = \frac{\boldsymbol{H}_{\mathcal{L}}^H\boldsymbol{\Delta}_{\mathcal{L}}}{\|\boldsymbol{H}_{\mathcal{L}}^H\boldsymbol{\Delta}_{\mathcal{L}}\|_F} \in \mathbb{C}^{U\times 2U}. \quad (26)$$

In summary, the MU-STLC transmitter transmits $\boldsymbol{S}$ in (8) using the MU-STLC preprocessing matrix $\boldsymbol{V}_o$ in (26), and user u obtain the estimates of $x_{u,1}$ and $x_{u,2}$, denoted by $\widetilde{x_{u,1}}$ and $\widetilde{x_{u,2}}$, respectively, as (from (15) and (17))

$$\begin{bmatrix}\widetilde{x_{u,1}}\\ \widetilde{x_{u,2}}\end{bmatrix} = c\left[\boldsymbol{I}_2\ \boldsymbol{Q}_2^T\right]\begin{bmatrix}\boldsymbol{r}_{u,1}\\ \boldsymbol{r}_{u,2}^*\end{bmatrix}, \quad (27)$$

which is the same as the conventional single-user STLC decoding process [1], [14]. Here, note that the effective channel gain, i.e., $1/c$, is not required to detect phase-shift keying (PSK) modulated symbols, whereas it needs to be estimated for the non-PSK modulated symbol detection. In other words, only partial CSI is required at the STLC users (receivers). The effective channel gain can be estimated through the blind estimation schemes [22]–[24] and/or a training-based machine learning algorithm [11].

IV. TRANSMIT ANTENNA SELECTION STRATEGIES

In the previous section, we design the MU-STLC preprocessing matrix. We now propose a TAS strategy that maximizes the detection SINR. To this end, we derive the detection SINR of the MU-STLC system using the optimal preprocessing $\boldsymbol{V}_o$ in (26). By substituting $\boldsymbol{W}_{t,o}$ in (23) into $\boldsymbol{W}_t$ in (21), the minimum MSE, denoted by J_{min}, is derived as follows:

$$\begin{aligned}J_{min} &= \mathrm{tr}\left(\sigma_x^2\left(\boldsymbol{H}_t\boldsymbol{W}_{t,o} - \boldsymbol{I}_{2U}\right)\left(\boldsymbol{W}_{t,o}^H\boldsymbol{H}_t^H - \boldsymbol{I}_{2U}\right) + 2U\sigma_z^2\boldsymbol{W}_{t,o}\boldsymbol{W}_{t,o}^H\right)\\ &= \mathrm{tr}\left(\sigma_x^2\left(\boldsymbol{W}_{t,o}^H\boldsymbol{H}_t^H - \boldsymbol{I}_{2U}\right)\left(\boldsymbol{H}_t\boldsymbol{W}_{t,o} - \boldsymbol{I}_{2U}\right) + 2U\sigma_z^2\boldsymbol{W}_{t,o}^H\boldsymbol{W}_{t,o}\right)\\ &= \mathrm{tr}\left(\left\{\sigma_x^2\left(\boldsymbol{W}_{t,o}^H\boldsymbol{H}_t^H - \boldsymbol{I}_{2U}\right)\boldsymbol{H}_t + 2U\sigma_z^2\boldsymbol{W}_{t,o}^H\right\}\boldsymbol{W}_{t,o} + \sigma_x^2\left(\boldsymbol{I}_{2U} - \boldsymbol{W}_{t,o}^H\boldsymbol{H}_t^H\right)\right)\\ &\overset{(a)}{=} \mathrm{tr}\left(\sigma_x^2\left(\boldsymbol{I}_{2U} - \boldsymbol{H}_t\boldsymbol{W}_{t,o}\right)\right)\\ &= \sigma_x^2\,\mathrm{tr}\left(\boldsymbol{\Delta}_{\mathcal{L}}^{-1}\boldsymbol{\Delta}_{\mathcal{L}} - \boldsymbol{H}_t\boldsymbol{H}_t^H\boldsymbol{\Delta}_{\mathcal{L}}\right)\\ &= \sigma_x^2\,\mathrm{tr}\left(\left(\boldsymbol{\Delta}_{\mathcal{L}}^{-1} - \boldsymbol{H}_t\boldsymbol{H}_t^H\right)\boldsymbol{\Delta}_{\mathcal{L}}\right)\\ &\overset{(b)}{=} \sigma_x^2\,\mathrm{tr}\left(\frac{2U\sigma_z^2}{\sigma_x^2}\boldsymbol{I}_{2U}\boldsymbol{\Delta}_{\mathcal{L}}\right)\\ &= 2U\sigma_z^2\,\mathrm{tr}\left(\boldsymbol{\Delta}_{\mathcal{L}}\right), \quad (28)\end{aligned}$$

$$\begin{aligned}J(\boldsymbol{W}_t) &= \mathrm{tr}\left(\mathrm{E}\left[\boldsymbol{e}\boldsymbol{e}^H\right]\right)\\ &= \mathrm{tr}\left(\mathrm{E}\left[\left((\boldsymbol{H}_t\boldsymbol{W}_t - \boldsymbol{I}_{2U})\boldsymbol{x} + \frac{1}{\sqrt{2}}\|\boldsymbol{W}_t\|_F\boldsymbol{z}'\right)\left((\boldsymbol{H}_t\boldsymbol{W}_t - \boldsymbol{I}_{2U})\boldsymbol{x} + \frac{1}{\sqrt{2}}\|\boldsymbol{W}_t\|_F\boldsymbol{z}'\right)^H\right]\right)\\ &= \mathrm{tr}\left(\mathrm{E}\left[\left((\boldsymbol{H}_t\boldsymbol{W}_t - \boldsymbol{I}_{2U})\boldsymbol{x} + \frac{1}{\sqrt{2}}\|\boldsymbol{W}_t\|_F\boldsymbol{z}'\right)\left(\boldsymbol{x}^H\left(\boldsymbol{W}_t^H\boldsymbol{H}_t^H - \boldsymbol{I}_{2U}\right) + \frac{1}{\sqrt{2}}\|\boldsymbol{W}_t\|_F\boldsymbol{z}'^H\right)\right]\right)\\ &= \mathrm{tr}\left(\mathrm{E}\left[(\boldsymbol{H}_t\boldsymbol{W}_t - \boldsymbol{I}_{2U})\boldsymbol{x}\boldsymbol{x}^H\left(\boldsymbol{W}_t^H\boldsymbol{H}_t^H - \boldsymbol{I}_{2U}\right)\right] + \mathrm{E}\left[(\boldsymbol{H}_t\boldsymbol{W}_t - \boldsymbol{I}_{2U})\boldsymbol{x}\frac{1}{\sqrt{2}}\|\boldsymbol{W}_t\|_F\boldsymbol{z}'^H\right]\right.\\ &\quad\left. + \mathrm{E}\left[\frac{1}{\sqrt{2}}\|\boldsymbol{W}_t\|_F\boldsymbol{z}'\boldsymbol{x}^H\left(\boldsymbol{W}_t^H\boldsymbol{H}_t^H - \boldsymbol{I}_{2U}\right)\right] + \mathrm{E}\left[\frac{1}{\sqrt{2}}\|\boldsymbol{W}_t\|_F\boldsymbol{z}'\frac{1}{\sqrt{2}}\|\boldsymbol{W}_t\|_F\boldsymbol{z}'^H\right]\right)\\ &= \mathrm{tr}\left((\boldsymbol{H}_t\boldsymbol{W}_t - \boldsymbol{I}_{2U})\mathrm{E}\left[\boldsymbol{x}\boldsymbol{x}^H\right]\left(\boldsymbol{W}_t^H\boldsymbol{H}_t^H - \boldsymbol{I}_{2U}\right) + \frac{1}{\sqrt{2}}(\boldsymbol{H}_t\boldsymbol{W}_t - \boldsymbol{I}_{2U})\|\boldsymbol{W}_t\|_F\,\mathrm{E}\left[\boldsymbol{x}\boldsymbol{z}'^H\right]\right.\\ &\quad\left. + \frac{1}{\sqrt{2}}\|\boldsymbol{W}_t\|_F\,\mathrm{E}\left[\boldsymbol{z}'\boldsymbol{x}^H\right]\left(\boldsymbol{W}_t^H\boldsymbol{H}_t^H - \boldsymbol{I}_{2U}\right) + \frac{1}{2}\|\boldsymbol{W}_t\|_F\|\boldsymbol{W}_t\|_F\,\mathrm{E}\left[\boldsymbol{z}'\boldsymbol{z}'^H\right]\right)\\ &= \mathrm{tr}\left(\sigma_x^2(\boldsymbol{H}_t\boldsymbol{W}_t - \boldsymbol{I}_{2U})\left(\boldsymbol{W}_t^H\boldsymbol{H}_t^H - \boldsymbol{I}_{2U}\right) + \sigma_z^2\|\boldsymbol{W}_t\|_F^2\boldsymbol{I}_{2U}\right)\\ &= \mathrm{tr}\left(\sigma_x^2(\boldsymbol{H}_t\boldsymbol{W}_t - \boldsymbol{I}_{2U})\left(\boldsymbol{W}_t^H\boldsymbol{H}_t^H - \boldsymbol{I}_{2U}\right) + 2U\sigma_z^2\boldsymbol{W}_t\boldsymbol{W}_t^H\right). \quad (21)\end{aligned}$$

where (a) comes from (22) and (b) follows the definition in (24). Consequently, the detection SINR is derived as follows:

$$\rho_{\mathcal{L}} = \frac{\mathrm{E}[\boldsymbol{x}^H \boldsymbol{x}]}{J_{min}} - 1 = \frac{\sigma_x^2}{\sigma_z^2 \,\mathrm{tr}\,(\boldsymbol{\Delta}_{\mathcal{L}})} - 1. \tag{29}$$

The TAS that maximizes the detection SINR in (29) is then designed by solving the following optimization problem:

$$\max_{\mathcal{L} \subset \mathcal{A}_M} \rho_{\mathcal{L}} \equiv \min_{\mathcal{L} \subset \mathcal{A}_M} \mathrm{tr}\,(\boldsymbol{\Delta}_{\mathcal{L}}), \tag{30}$$

where $\mathcal{A}_M$ is the set of all possible selected antenna combinations $\mathcal{L}$ from M transmit antennas, for example, $\mathcal{A}_4 = \{\{1, 2\}, \{1, 3\}, \{1, 4\}, \{2, 3\}, \{2, 4\}, \{3, 4\}\}$ when $M = 4$ and $U = 2$.

In general, for M transmit antennas,

$$\binom{M}{U} = \frac{M(M-1) \times \cdots \times (M-U+1)}{U!}$$

combinations are possible for the TAS pairs. Since $\mathcal{O}(M^3)$-complexity is typically required to compute (29), the overall computational complexity of the proposed TAS is $\mathcal{O}(M^{U+3})$, which is prohibitive if M is massive.

To reduce the TAS complexity, the channel-norm (CN)-based greedy TAS algorithm shown in Algorithm 1 can be considered.

Algorithm 1 Channel-Norm-Greedy-Based TAS Algorithm

1. Initialization: $\mathcal{L} = \emptyset$ and $\mathcal{M} = \{1, \ldots, M\}$
2. **for** $u = 1 : U$ **do**
3. Find the antenna that has the strongest norm of the channel vector $\boldsymbol{h}_m$, such that $m = \arg\max_{m \in \mathcal{M}} \|\boldsymbol{h}_m\|$
4. Update the selected antenna set: $\mathcal{L} = \mathcal{L} \cup \{m\}$
5. Update the antenna set: $\mathcal{M} = \mathcal{M} \setminus \{m\}$
6. **end for**

The norm of the $2U$-by-1 channel vector for all $m \in \mathcal{M}$, i.e., $\|\boldsymbol{h}_m\|, \forall m \in \mathcal{M}$, is required for Algorithm 1, and thus the computational complexity is $\mathcal{O}(UM)$. Although the computational complexity can be significantly reduced by the CN-based greedy TAS algorithm compared to the optimal TAS strategy in (30), the performance improvement of the TAS is marginal as shown in Section V. To further improve the TAS gain, we propose a novel greedy algorithm that initially selects the transmit antenna with the largest $\|\boldsymbol{h}_m\|$ and then iteratively finds the antenna minimizing the trace of MSE (or equivalently maximizing the detection SINR) from remaining transmit antennas in each greedy step. The proposed SINR-based greedy TAS algorithm is summarized in Algorithm 2.

Next, we consider the computational complexity of Algorithm 2. For the ith greedy step, (24) in line 8 needs to be computed $|\mathcal{M}|$ times, and each calculation has a complexity of $\mathcal{O}(U^3)$ since $\boldsymbol{H}_{\mathcal{L}'}$ is a $2U$-by-i matrix. Noting that

Algorithm 2 SINR-Greedy-Based TAS Algorithm

1. Initialization: $\mathcal{L} = \emptyset$ and $\mathcal{M} = \{1, \ldots, M\}$
2. The same as procedure 3 of Algorithm 1
3. Update the selected antenna set: $\mathcal{L} = \mathcal{L} \cup \{m\}$
4. Update the antenna set: $\mathcal{M} = \mathcal{M} \setminus \{m\}$
5. **for** $i = 1 : U - 1$ **do**
6. **for** $m = 1 : |\mathcal{M}|$ **do**
7. Construct a partial channel matrix: $\boldsymbol{H}_{\mathcal{L}'} \triangleq [\boldsymbol{H}_{\mathcal{L}}\ \boldsymbol{h}_{\mathcal{M}(m)}] \in \mathbb{C}^{2U \times (i+1)}$, where $\mathcal{M}(m)$ is the mth element of $\mathcal{M}$
8. Compute $\boldsymbol{\Delta}_{\mathcal{L}'}$ using $\boldsymbol{H}_{\mathcal{L}'}$ in (24).
9. $cost(m) = \mathrm{tr}(\boldsymbol{\Delta}_{\mathcal{L}'})$
10. **end for**
11. Select an antenna index: $m^* = \arg\min_m \, cost(m)$
12. Update the selected antenna set: $\mathcal{L} = \mathcal{L} \cup \{\mathcal{M}(m^*)\}$
13. Update the antenna set: $\mathcal{M} = \mathcal{M} \setminus \{\mathcal{M}(m^*)\}$
14. **end for**

$|\mathcal{M}| = M - i - 1$ in the ith greedy step, the upper bound of the overall computational complexity is given by

$$\begin{aligned}
&\mathcal{O}\left(\sum_{i=1}^{i=U-1} (M-i-1)(2U)^3 \right) \\
&= \mathcal{O}\left(U^3(2MU - M - U - U^2 + 2) \right) \\
&\lessapprox \mathcal{O}\left(MU^4 \right) \\
&\overset{(a)}{\leq} \mathcal{O}\left(M^5 \right),
\end{aligned} \tag{31}$$

where (a) comes from the fact that the maximum supportable number of users is limited by $M/2$, i.e., $U \leq M/2$.

V. PERFORMANCE EVALUATION AND DISCUSSION

In this section, we compare the performance of various schemes that can support multiple users. In the first part, the received SINRs of multiuser STLC schemes are compared. In the second part, the computational complexity of the SINR-greedy TAS and optimal TAS methods are compared for the proposed MU-STLC scheme. In the last part, BERs of the proposed MU-STLC and the conventional space-division multiple access (SDMA) schemes in [25]–[27] are compared.

A. SINR COMPARISON

The transmitter has M transmit antennas to support U users ($M \geq U$). For the TAS schemes, the proposed SINR-greedy TAS scheme is compared to a random TAS scheme, CN-greedy scheme, and optimal TAS scheme. Furthermore, we compare the received SINRs of the proposed MU-STLC scheme and the existing STLC scheme in [2]. The compared systems are summarized as follows:

- $(M \rightarrow U) \times 2U$ MU-STLC w/ random TAS: This is an MU-STLC system, where U transmit antennas are randomly selected from M antennas for MU-STLC.

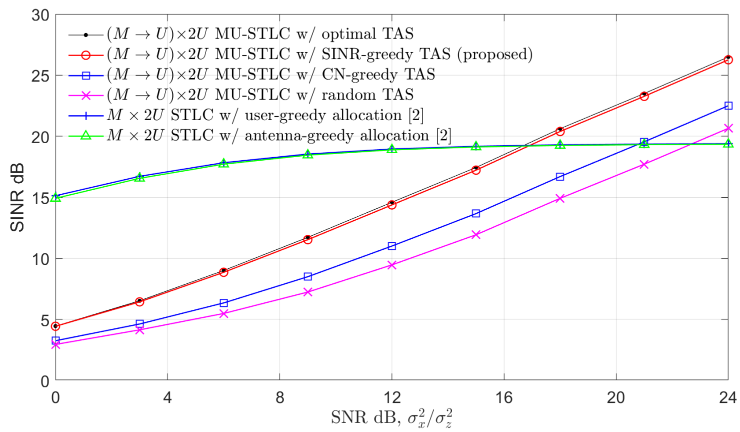

FIGURE 4. SINR of multiuser STLC schemes when $M = 80$ and $U = 2$. '$(M \to U)$' represents that U transmit antennas are selected from M antennas.

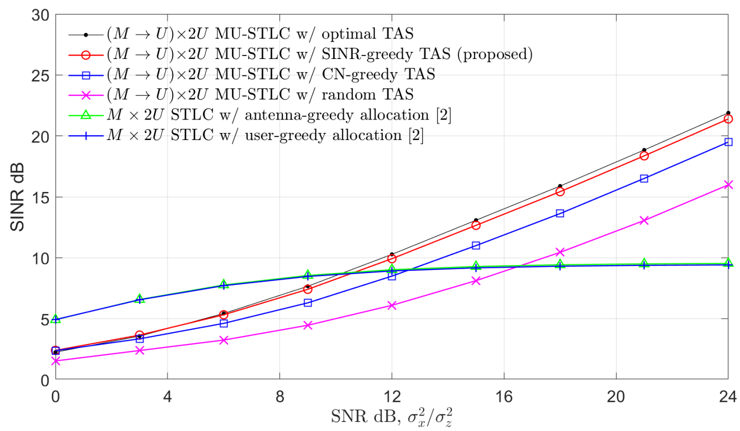

FIGURE 5. SINR of multiuser STLC schemes when $M = 8$ and $U = 2$. '$(M \to U)$' represents that U transmit antennas are selected from M antennas.

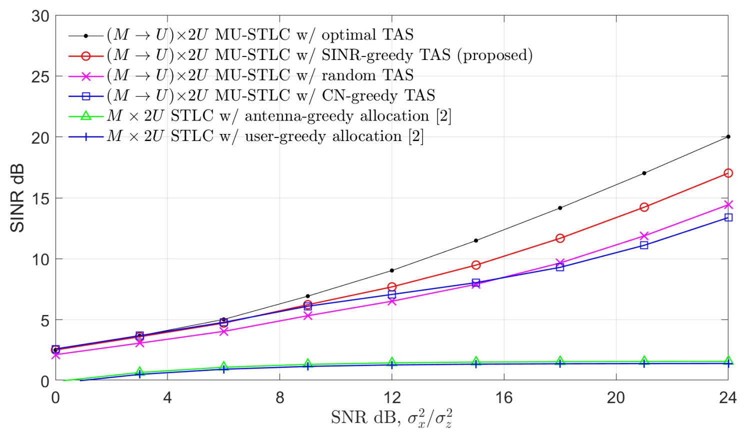

FIGURE 6. SINR of multiuser STLC schemes when $M = 8$ and $U = 4$. '$(M \to U)$' represents that U transmit antennas are selected from M antennas.

- $(M \to U) \times 2U$ MU-STLC w/ CN-greedy TAS: Channel-norm-based greedy (CN-greedy) algorithm, i.e., Algorithm 1, is used to select U transmit antennas from M for MU-STLC.
- $(M \to U) \times 2U$ MU-STLC w/ SINR-greedy TAS: SINR-based greedy (SINR-greedy) algorithm, i.e., Algorithm 2, is used to select U transmit antennas from M antennas for MU-STLC.

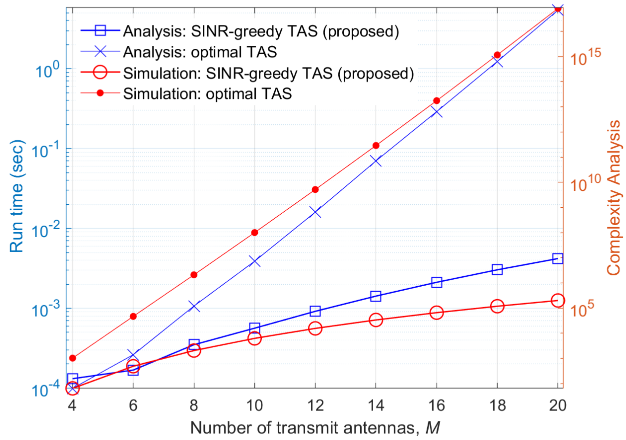

FIGURE 7. Complexity of MU-STLC in a log scale when over M when $U = M/2$.

- $(M \to U) \times 2U$ MU-STLC w/ optimal TAS: U transmit antennas are optimally selected from M antennas for MU-STLC by solving (30).
- $M \times 2U$ STLC w/ antenna-greedy allocation [2]: Transmit antennas are allocated to each user to maximize SINR in each greedy step. In each greedy step, M/U antennas are allocated to one specific user.
- $M \times 2U$ STLC w/ user-greedy allocation [2]: U antennas are allocate to U users to maximize SINR in each greedy step. The greedy steps are repeated until M/U antennas are allocated to each user.

Channels and noises are generated according to the signal model in (10) of Section III.

In Fig. 4, the SINRs are evaluated over the SNR, i.e., σ_x^2/σ_z^2, when the numbers of transmit antennas and users are 80 and 2, respectively, namely, $M = 80$ and $U = 2$. Here, it is shown that the proposed MU-STLC w/ SINR-greedy scheme achieves near-optimal TAS performance. However, the performance of a CN-greedy TAS scheme is similar to that of a random TAS scheme. This implies that the CN-greedy does not capture the multiuser interference effectively. On the other hand, the conventional multiuser STLC scheme in [2] outperforms the proposed MU-STLC scheme when SNR is low, however, the SINR of the conventional multiuser STLC scheme is saturated as SNR increases. Furthermore, note that the conventional multiuser STLC scheme uses the whole transmit antennas, i.e., M, whereas the proposed MU-STLC uses U selected transmit antennas.

In Fig. 5, the SINRs are compared when the number of transmit antennas is small, i.e., $M = 8$. In general, the SINRs of all schemes decrease as M decreases. Here, the SINR achieved by the proposed MU-STLC with SINR-greedy TAS scheme is slightly lower than the MU-STLC with optimal TAS scheme. However, the SINR of the conventional multiuser STLC decreases significantly, approximately 10 dB. This is because the multiuser STLC schemes in [2] do not consider multiuser (inter-stream) interferences, thus the insufficient number of transmit antennas cannot effectively suppress the multiuser interferences. As the number of users increases to $U = 4$, the conventional multiuser STLC schemes do not achieve comparable performance to the proposed MU-STLC schemes as shown in Fig. 6.

B. COMPLEXITY COMPARISON OF TAS METHODS

As shown in Fig. 7, where the run time is shown in log scale, the complexity of the optimal TAS increases exponentially as M increases when $U = M/2$. On the other hand, the complexity of the proposed SINR-based greedy TAS increases moderately. As observed here, the complexity increases as M increases and the complexity analyses match well with the numerical results.

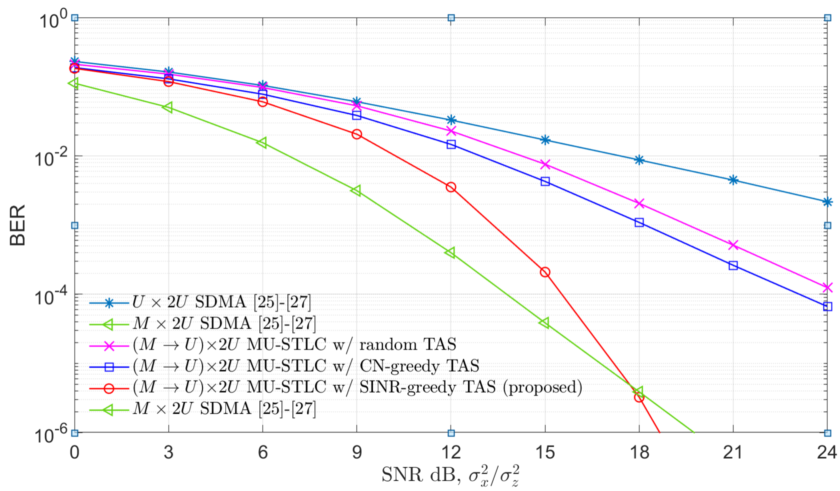

FIGURE 8. BER for QPSK over SNR when $M = 8$ and $U = 4$. '$(8 \to 4)$' represents that four transmit antennas are selected from eight antennas.

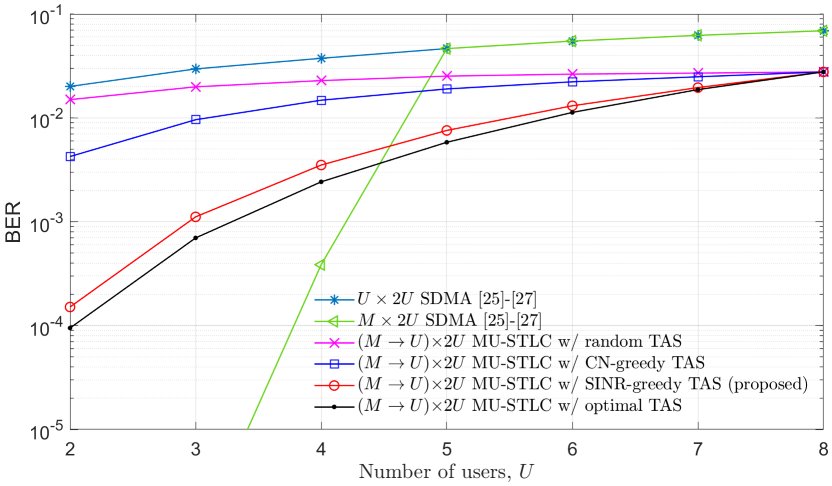

FIGURE 9. BER for QPSK over U when $M = 8$ and SNR $\sigma_x^2/\sigma_z^2 = 12$ *dB*. '$(M \to U)$' represents that U transmit antennas are selected from M antennas.

C. BER COMPARISON

BER is evaluated for verifying the proposed SINR-based greedy TAS, where the proposed MU-STLC transmitter has eight transmit antennas to support U users ($M = 8 \geq U$), and QPSK is employed. For the BER comparison, we consider two SDMA schemes in [25]–[27]. One SDMA scheme uses U transmit antennas, for the fair comparison with the MU-STLC using U selected antennas. The other SDMA scheme uses M transmit antennas.

In Fig. 8, the BER performance is compared across the system SNR, i.e., σ_x^2/σ_z^2, when $U = 4$. From the results, we can observe that the performance improvement from the CN-based greedy TAS is marginal. On the other hand, the proposed SINR-based greedy TAS achieves near-optimal performance. The 4×8 SDMA achieves poor performance due to the lack of the degree of freedom for beamforming after the spatial division as $U > M/2$. Note that 8×8 SDMA achieves the best performance, yet it uses eight transmit antennas (not four) and full CSI at both transmitter and receiver. Even though the SINR-based TAS STLC uses four selected antennas, it outperforms the 8×8 SDMA system in the high-SNR regime due to the antenna selection diversity.

In Fig. 9, the BERs are evaluated across U when $M = 8$ and the SNR is 10 dB. Due to the increase of the multiuser interference, the BER performance is degraded for all schemes as U increases. The proposed SINR-based TAS outperforms $M \times 2U$ SDMA when $U > M/2$. It is verified that the TAS can improve BER performance regardless of the number of users. Furthermore, the proposed SINR-based greedy TAS achieves near-optimal performance with significantly reduced computational complexity. In Fig. 7, the complexity analyses in Section IV are verified by comparing with run-time simulation results.

VI. CONCLUSION

In this study, we designed an MU-STLC system supporting multiple STLC users, and then proposed a novel SINR-based greedy TAS scheme. The proposed method significantly improves the BER performance at the cost of a moderate increase in the computational load. The proposed MU-STLC can be applied to a multiuser multi-antenna system requiring low-complexity and low-cost user devices.

REFERENCES

[1] J. Joung, "Space–Time line code," *IEEE Access*, vol. 6, pp. 1023–1041, 2018.

[2] J. Joung, "Space–Time line code for massive MIMO and multiuser systems with antenna allocation," *IEEE Access*, vol. 6, pp. 962–979, 2018.

[3] V. Tarokh, N. Seshadri, and A. R. Calderbank, "Space-time codes for high data rate wireless communication: Performance criterion and code construction," *IEEE Trans. Inf. Theory*, vol. 44, no. 2, pp. 744–765, Mar. 1998.

[4] V. Tarokh, H. Jafarkhani, and A. R. Calderbank, "Space-time block codes from orthogonal designs," *IEEE Trans. Inf. Theory*, vol. 45, no. 5, pp. 1456–1467, Jul. 1999.

[5] V. Tarokh, H. Jafarkhani, and A. R. Calderbank, "Space-time block coding for wireless communications: Performance results," *IEEE J. Sel. Areas Commun.*, vol. 17, no. 3, pp. 451–460, Mar. 1999.

[6] S. M. Alamouti, "A simple transmitter diversity scheme for wireless communications," *IEEE J. Sel. Areas Commun.*, vol. 16, no. 8, pp. 1451–1458, Oct. 1998.

[7] J. Joung and E.-R. Jeong, "Multiuser Space–Time line code with optimal and suboptimal power allocation methods," *IEEE Access*, vol. 6, pp. 51766–51775, 2018.

[8] J. Joung, "Energy efficient Space–Time line coded regenerative two-way relay under per-antenna power constraints," *IEEE Access*, vol. 6, pp. 47026–47035, 2018.

[9] J. Joung and J. Choi, "Space–Time line codes with power allocation for regenerative two-way relay systems," *IEEE Trans. Veh. Technol.*, vol. 68, no. 5, pp. 4884–4893, May 2019.

[10] J. Joung and J. Choi, "Uneven power amplifier shuffling for space-time line code systems," *IEEE Access*, vol. 6, pp. 58491–58500, 2018.

[11] J. Joung and B. C. Jung, "Machine learning based blind decoding for Space–Time line code (STLC) systems," *IEEE Trans. Veh. Technol.*, vol. 68, no. 5, pp. 5154–5158, May 2019.

[12] C. Wu, Y. Xiao, Y. L. Guan, J. Wang, X. Li, and P. Yang, "Space-Time/Frequency line coded OFDM: System design and practical implementation," *IEEE Access*, vol. 7, pp. 151915–151928, 2019.
[13] J. Joung, J. Choi, B. C. Jung, and S. Yu, "Artificial noise injection and its power loading methods for secure space-time line coded systems," *Entropy*, vol. 21, no. 5, p. 515, 2019.
[14] J. Joung, J. Choi, and B. C. Jung, "Double space-time line codes," *IEEE Trans. Veh. Technol.*, vol. 69, no. 2, pp. 2316–2321, Feb. 2020.
[15] R. W. Heath and D. J. Love, "Multimode antenna selection for spatial multiplexing systems with linear receivers," *IEEE Trans. Signal Process.*, vol. 53, no. 8, pp. 3042–3056, Aug. 2005.
[16] S. K. Mishra and K. D. Kulat, "Reduced feedback rate schemes for transmit antenna selection with Alamouti coding," *IEEE Access*, vol. 6, pp. 10028–10040, 2018.
[17] H. Alves, M. De Castro Tome, P. H. J. Nardelli, C. H. M. De Lima, and M. Latva-Aho, "Enhanced transmit antenna selection scheme for secure throughput maximization without CSI at the transmitter," *IEEE Access*, vol. 4, pp. 4861–4873, 2016.
[18] S. Asaad, A. Bereyhi, A. M. Rabiei, R. R. Muller, and R. F. Schaefer, "Optimal transmit antenna selection for massive MIMO wiretap channels," *IEEE J. Sel. Areas Commun.*, vol. 36, no. 4, pp. 817–828, Apr. 2018.
[19] H. Lei, J. Zhang, K.-H. Park, P. Xu, I. S. Ansari, G. Pan, B. Alomair, and M.-S. Alouini, "On secure NOMA systems with transmit antenna selection schemes," *IEEE Access*, vol. 5, pp. 17450–17464, 2017.
[20] R. Rajashekar, K. V. S. Hari, and L. Hanzo, "Transmit antenna subset selection in spatial modulation relying on a realistic error-infested feedback channel," *IEEE Access*, vol. 6, pp. 5879–5890, 2018.
[21] L. Zhu, J. Zhu, S. Wang, and J. Zhang, "Adaptive transmit antenna selection based on PCA for millimeter wave LOS MIMO channel," *IEEE Access*, vol. 7, pp. 12087–12096, 2019.
[22] P. Gao and C. Tepedelenlioglu, "SNR estimation for nonconstant modulus constellations," *IEEE Trans. Signal Process.*, vol. 53, no. 3, pp. 865–870, Mar. 2005.
[23] F. Bellili, A. Stephenne, and S. Affes, "Cramer-Rao lower bounds for NDA SNR estimates of square QAM modulated transmissions," *IEEE Trans. Commun.*, vol. 58, no. 11, pp. 3211–3218, Nov. 2010.
[24] F. Bellili, A. Methenni, and S. Affes, "Closed-form CRLBs for SNR estimation from turbo-coded BPSK-, MSK-, and Square-QAM-Modulated signals," *IEEE Trans. Signal Process.*, vol. 62, no. 15, pp. 4018–4033, Aug. 2014.
[25] Z. Pan, K.-K. Wong, and T.-S. Ng, "Generalized multiuser orthogonal space-division multiplexing," *IEEE Trans. Wireless Commun.*, vol. 3, no. 6, pp. 1969–1973, Nov. 2004.
[26] Q. H. Spencer, A. L. Swindlehurst, and M. Haardt, "Zero-forcing methods for downlink spatial multiplexing in multiuser MIMO channels," *IEEE Trans. Signal Process.*, vol. 52, no. 2, pp. 461–471, Feb. 2004.
[27] L.-U. Choi and R. D. Murch, "A transmit preprocessing technique for multiuser MIMO systems using a decomposition approach," *IEEE Trans. Wireless Commun.*, vol. 3, no. 1, pp. 20–24, Jan. 2004.

JINGON JOUNG (Senior Member, IEEE) received the B.S. degree in radio communication engineering from Yonsei University, Seoul, South Korea, in 2001, and the M.S. and Ph.D. degrees in electrical engineering and computer science from KAIST, Daejeon, South Korea, in 2003 and 2007, respectively.

He was a Postdoctoral Fellow with KAIST, and UCLA, CA, USA, in 2007 and 2008, respectively. He was a Scientist with the Institute for Infocomm Research, Agency for Science, Technology and Research (A*STAR), Singapore, from 2009 to 2015, and joined Chung-Ang University (CAU), Seoul, South Korea, in 2016, as a Faculty Member. He is currently an Associate Professor with the School of Electrical and Electronics Engineering, CAU, where he is also the Principal Investigator of the Intelligent Wireless Systems Laboratory. His research interests include wireless communication signal processing, numerical analysis, algorithms, and machine learning.

Dr. Joung was a recipient of the First Prize of the Intel-ITRC Student Paper Contest, in 2006. He was recognized as the Exemplary Reviewers of the IEEE Communications Letters, in 2012, and the IEEE Wireless Communications Letters, in 2012, 2013, 2014, and 2019. He has served as the Guest Editor for IEEE Access, in 2016, as the Editorial Board Member of the *APSIPA Transactions on Signal and Information Processing*, from 2014 to 2019, and as a Guest Editor for the *MDPI Electronics*, in 2019. He is serving as the Associate Editor for the IEEE Transactions on Vehicular Technology and *MDPI Sensors*.

JIHOON CHOI (Senior Member, IEEE) received the B.S., M.S., and Ph.D. degrees from KAIST, Daejeon, South Korea, in 1997, 1999, and 2003, respectively.

From 2003 to 2004, he was with the Department of Electrical and Computer Engineering, The University of Texas at Austin, where he performed research on MIMO-OFDM systems as a Postdoctoral Fellow. From 2004 to 2008, he was with the Samsung Electronics, South Korea, where he worked on developments of radio access stations for M-WiMAX and base stations for CDMA 1xEV-DO Rev.A/B. In 2008, he joined Korea Aerospace University (KAU), Goyang, South Korea, as a Faculty Member. He is currently a Professor with the School of Electronics and Information Engineering, KAU, where he is also the Chief Investigator of the Intelligent Signal Processing Laboratory. His research interests include MIMO communication techniques, signal processing algorithms, secure transmission in the physical layer, radar signal processing, and modem design for future cellular networks, wireless LANs, the IoT devices, and digital broadcasting systems.